Journal of MATERIALS RESEARCH

Article
DOI: 10.1557/jmr.2019.197

BUILDING ADVANCED MATERIALS VIA PARTICLE AGGREGATION AND MOLECULAR SELF-ASSEMBLY

FOCUS ISSUE

A novel and facile way to synthesize diamondoids nanowire cluster array

Jilong Wang[1], Jingjing Qiu[2,a)], Shiren Wang[3,b)]

[1]Key Laboratory of Textile Science & Technology of Ministry of Education, College of Textiles, Donghua University, Shanghai 201620, People's Republic of China; and Department of Mechanical Engineering, Texas Tech University, Lubbock, Texas 79409, USA
[2]Department of Mechanical Engineering, Texas Tech University, Lubbock, Texas 79409, USA
[3]Department of Materials Science and Engineering, Texas A&M University, Texas 77843-3131, USA
[a)]Address all correspondence to these authors. e-mail: jenny.qiu@ttu.edu
[b)]e-mail: s.wang@tamu.edu

Received: 9 April 2019; accepted: 15 May 2019

Nowadays, hierarchical materials have received tremendous interests because of their unique physical and chemical properties. In this article, a novel and facile particle aggregation method was used to fabricate vertically aligned diamondoid nanowires and hierarchical branched nanowire cluster array by using an electrophoresis template method. Triamantane, a three-cage diamondoid, was applied as raw material in current research. Diamondoids are nanometer-sized, hydrogen-terminated diamond-like, saturated hydrocarbons, which process great potential in nanotechnology due to biocompatibility and ultrahard nature. By electrophoresis template method, triamantane molecules dissolved in toluene were transferred into a porous alumina template by electric field and form the one-dimensional (1D) nanostructure with high aspect ratio. After that, a two-step thermal treatment was applied to the nanowires to achieve hierarchical branched nanowires. The surface morphologies of triamantane nanowire array with different treatments were characterized by scanning electron microscopy. This approach opens a new avenue for mass production of the vertically aligned diamondoid nanowires and hierarchical branched nanowire cluster arrays.

Introduction

In the modern nanoscience, diamondoids, novel carbon-based functional nanostructures, have recently received tremendous interests. Diamondoids (or diamond molecules) are nanometer-sized, hydrogen-terminated diamond–like, saturated hydrocarbons [1], which process great potential in nanotechnology like its cousins graphene, carbon dots, and nanodiamond [2, 3, 4, 5], such as drug delivery, DNA delivery, nanorobotics, and nanolubrication [6], since diamondoids are biocompatible and ultrahard. Adamantane, amine-derivatives of the lower diamondoid, has been employed in pharmaceutical applications as antiviral and anti-Parkinson's agents [7]. Diamondoids consisting of different numbers of diamond–crystal cages own a large variety of size and can easily be chemically modified [8], which can be used to tune the optical and electronic properties [9]. For example, diamondoids can be chemically connected onto metallic surface by thiol groups to form a self-assembled layer, which process a negative electron affinity (NEA) and a strong monochromatic emission [1]. Theoretically, a larger interlinked nanostructure can be fabricated from the lower diamondoids and their derivatives [10]. Adamantane, a cycloalkane with formula $C_{10}H_{16}$, is the smallest diamondoid, which the carbon atoms of adamantane are sp^3 bonded to form a cage in the diamond lattice [11]. Diamantane $C_{14}H_{20}$ and triamantane $C_{18}H_{24}$ are generated by fusing two and three adamantine cages together, respectively. These structures are called lower molecules and their sizes are smaller than 1 nm. The rest of entire diamondoid series consists of increasing number of cages, which processes multiple isomers for a given number of cages [12]. In 2002, Dahl et al. reported that higher diamondoids containing four to eleven cages ranged in the size of 1–2 nm [13], which were isolated from petroleum and then purified by pyrolysis and chromatography.

Traditional one-dimensional (1D) fiber material is in micro scale, which is employed in wide range [14]. Now tremendous attempts have been devoted to achieve 1D nanomaterials, such as carbon nanotubes, carbon nanofibers, and diamond nanowires [15]. Because of superior properties, 1D organic

https://doi.org/10.1557/jmr.2019.197 Published online by Cambridge University Press

© Materials Research Society 2019

nanostructures have attracted lots of interests [16]. Especially, by combing the variety of 1D nanostructure, the 1D nanomaterials own large numbers of promising electronic, optical, and optoelectronic applications in photovoltaics, nanophotonics, nanoelectronics, and sensing [17]. Diamond nanowires process theoretically higher aspect ratio than zero dimensional (0D) diamond nanoparticles [18], which are attracting a large number of interests. The traditional way to obtain diamond nanowires is top–down etching, briefly, bulk diamond crystal film was masked, and continually etched by plasma to produce vertically aligned diamond nanowires [19]. Chemical vapor deposition (CVD) is the second type to produce one-dimensional (1D) diamond nanowires [20]. However, both two methods need complicated and expensive facilities and processes compared to other 1D material, like carbon nanotubes [21], nanofibers [22], and metal nanowires [23].

Particle aggregation refers to formation in a suspension by destabilization of colloidal systems, which is widely applied and studied [24, 25]. During this destabilization process, particles that are well dispersed in the liquid phase contact to each other to spontaneously form aggregates. By this method, particle aggregation has been formed, it is not easily broken, which means it is normally an irreversible process. Usually, particle aggregates to the bottom of the container as sedimentation, which limits its application in specific nanostructure fabrication.

Diamondoids, like diamond, are NEA material [1], which can be used to prepare nanostructure through cathodic electrophoretic deposition (EPD) [26]. Previous studies presented that the diamond nanostructures were successfully produced by cathodic EPD [18]. However, to the best of our knowledge, no solution method has been applied to fabricate vertical diamondoid nanowires and orderly diamondoid nanocluster array. Electrophoresis with template is one of the most efficient and simple methods for synthesizing hierarchical branched nanostructures [27]. In addition, complicated 1D nanostructures, like branched nanostructures have attracted numerous of interests due to great function [28]. Various techniques have been developed to achieve different type hierarchical branched nanostructures; however, the complicated manufacturing processes severely limit their application [29]. Therefore, exploring a simple method to achieve hierarchical branched nanostructures is a great challenge.

In the current study, triamantane was used to achieve diamondoid nanowires through porous anodic aluminum oxide (AAO) film (as shown in Fig. S1). By introducing electric field, the diamondoid molecules were forced into the AAO cylindrical holes to form one-dimensional (1D) nanowires. A critical point drying process is necessary to obtain vertical diamondoid nanowires. The diamondoid nanowire bundles were fabricated without critical point drying process. To well improve the mechanical properties of diamondoid nanowire, two different heating processes were employed. After a two-step thermal treatment, the orderly diamondoid nanoclusters consisting of hierarchical branched nanowires were achieved, whereas a one-step thermal method failed with collapsed diamondoid nanowires. In addition, the mechanism of diamondoid nanowire/nanotube formation and simple explanation of hierarchical branched diamondoid nanowires formation were introduced. This approach opens a new pathway to assemble diamondoid nanowires array and branched nanowire cluster, which can be employed for applications in chemical sensors, light energy conversion devices, and nanoscale electronic and optoelectronic devices [30, 31, 32, 33]. The synthesized nanostructures with high aspect ratio can be used in dynamic tuning of surface wetting, drug delivery, immunoassay chips, MEMS actuators, field emission, and superhydrophobic surface [34].

Results and discussion

In this article, the triamantane was achieved from the higher diamondoids which is developed by Dr. Jeremy Dahl. The obtained triamantane was first characterized by a TA Q20 (TA Instruments Inc., New Castle, DE) to perform differential scanning calorimetry (DSC). As shown in Fig. S2, two peaks were observed in the DSC curve. One peak at 156 °C was resulted from the solid–solid transition of the diamond crystals. The peak at 225 °C was derived from the melting transition of the diamond crystals, which is similar to the previous literature [35].

To achieve diamondoids nanowire array, triamantane was used as raw material in this study. The triamantane discovered by Dr. Jeremy Dahl was first well dispersed in toluene by bath sonication for 15 min. Then the electrophoresis process was employed when an AAO film–attached silicon substrate was connected as a working electrode (as shown in Fig. S1). At the electrophoresis parameter of 30 V, 1 mA and one-hour continuous deposition, solid diamondoid nanowires were produced. After fabrication, the AAO template was etched by 1 M sodium hydroxide solution and dried via a heating plate; the surface morphology and structure of as-prepared diamondoid nanowires were characterized by scanning electron microscopy (SEM) via Hitachi S-4300 (Hitachi Appliances Inc., Tokyo, Japan), and SEM images are depicted in Fig. 1. Without critical point drying and thermal heating, diamondoid nanowires with unique diameter randomly laid on the silicon substrate, leading to failure of achieving vertically standing diamond nanowire array, because of the residual stress during dry process. As shown in Fig. 1(a), the curving diamondoid nanowires wrap each other to form nanowire bundles, which presented random diamondoid nanostructures that limit its further application in

https://doi.org/10.1557/jmr.2019.197 Published online by Cambridge University Press

© Materials Research Society 2019

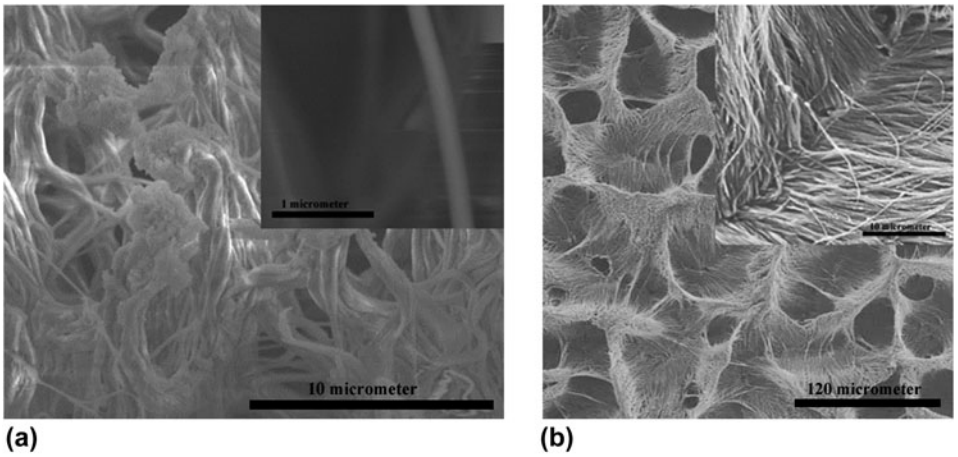


Figure 1: SEM images of (a) random twisted diamondoid nanowires, and the inset is individual diamondoid nanowire without critical point drying and heating treatment; (b) SEM images and magnified SEM images (the inset) of diamondoid nanowires with critical point drying and one-step heating treatment.

electronic devices. In addition, a knot without specific geometry was clearly observed on the top of each bundle, which might be the residual alumina that has not been removed by sodium hydroxide. An individual diamondoid nanowire is presented in the inset figure of Fig. 1(a). The diameter of diamondoid nanowires was exactly 200 nm, which is reasonable that the size of diamondoid nanowire is determined by the pore size on the AAO template. The surface of diamondoid nanowires was very smooth, which demonstrates that the particle aggregation of triamantane is successful and the size of triamantane is very small.

To achieve vertically aligned diamondoid nanowire array, critical point drying was employed to remove solvent to ensure that nanowires would not fall. After fabrication, the AAO template was etched by 1 M sodium hydroxide solution, and then critical point drying was employed to achieve vertically aligned diamondoid nanowires. Briefly, a series of mixture of water/ethanol (90/10, 70/30, 50/50, 30/70, 20/80, 10/90, and 0/100) with small ethanol concentration gradient were used in the solvent exchange process. Finally, the aqueous solution was exchanged by 100% ethanol and the 100% ethanol was removed by critical point drying instrument. As shown in Fig. S3, although the diamondoid nanowires were clearly separated, and not twisted to form nanobundles, the nanowires were not perfectly vertically aligned and the displacement between two nanowires nearly existed, which indicated the modulus of the diamondoid nanowires was low and the potential to form branched nanostructures after heat treatment. The diameter of diamondoid nanowires was also around 200 nm, which is derived from the pore size of the AAO template.

To well improve the mechanical property of the nanowires and to form specific diamondoid branched nanostructure array, two different heating treatments were performed. In one-step method, the nanowires were heated by a single-stage heating process at 226.5 °C for 1 h, which is 5 °C higher than the melting point of triamantane based on the DSC thermograms of the triamantane [35]. The morphology of nanostructure was characterized via SEM. As shown in Fig. 1(b), the diamondoid nanowires combined each other and collapsed without specific structure. In addition, after heating treatment, residual stress was left on the nanowires. As shown in the inset figure of Fig. 1(b), in each individual nanowire, lots of bubbles exist and they are not homogeneously distributed, which demonstrated that this approach had failed.

To form specific diamondoid nanostructure array, a two-step thermal treatment was performed to achieve orderly diamondoid branched nanostructures array and to remove the residual stress. As shown in Fig. 2(a), orderly nanocluster arrays were obtained on the silicon substrate, although the nanoclusters were not perfectly in the same size and the distances between nanoclusters were not uniform. The vertical nanoclusters consisting several triamantane nanowires are shown in a large size, which were much better than the collapsed nanowires and could be used in electronic field. It also presented that aligned nanowires could be achieved when the synthesis height is around 10 μm. To understand more detailed morphology information about the triamantane nanoclusters, a single nanocluster was amplified. As shown in Fig. 2(b), it was observed that the length of triamantane nanowires in the nanocluster was not the same, several nanowires around the core of nanocluster was much shorter than that in the core. The reason might be that the high heating temperature induced that some nanowires and some parts of nanowire were damaged. In addition, the bottom of diamondoid nanowires connected each other, which indicates that the nanowire cluster array was achieved with a hierarchical and branched structure. Fig. 2(b) also showed the top of nanoclusters with residual alumina oxide. Some long nanowires

https://doi.org/10.1557/jmr.2019.197 Published online by Cambridge University Press

© Materials Research Society 2019

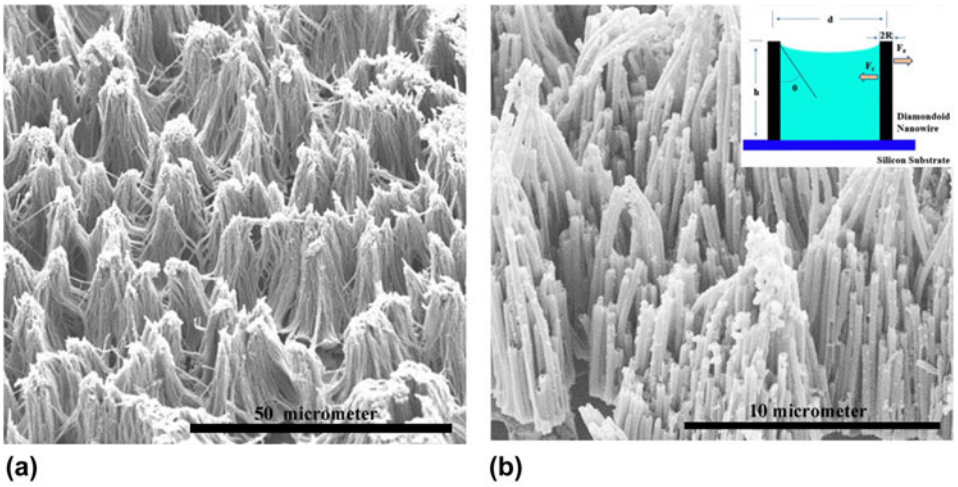


Figure 2: (a) SEM image of diamondoid nanowire cluster after two-step heating treatment; (b) amplified SEM image of diamondoid nanowire cluster, and the inset is schematic illustration of the driving force in clustering.

were still depicted in a collapsed state, which demonstrates the heating treatment could not successfully improve the modulus of triamantane nanowires. The inset figure of Fig. 2(b) presented the schematic illustration of the forces acting on the two neighboring diamondoid nanowires, where d stands for the distance between two nanowires, h for the height of nanorod, θ is the static contact angle of solvent on flat diamondoid nanowire surface, R is the radius of nanorod. Fe is the elastic resistant force to endure bending or distortion, which is proportional to the Young's modulus of diamondoid nanowire, while inversely proportional to the cube of nanowire height. Due to the low Young's modulus and large height (60 μm), the Fe is tiny in this diamondoid nanowire system, which cannot withstand the large capillary force F_c, leading to the collapse of diamondoid nanowires into the nanocluster structure. To further develop the vertically aligned diamondoid nanowires, the modulus and length of nanowires should be carefully designed.

As shown in Fig. 3(a), diamondoid nanotubes were clearly found, which indicates that the diamondoid continuously diffused into the hole and deposited. According to the nanostructure of the 1D diamondoid nanowire/nanotube depicted in the SEM images, a detailed synthesis mechanism is presented in Fig. 3(b). The synthesis mechanism may not be similar to our previous work where acid-treated diamond nanoparticles containing electron-defect carboxyl and hydroxyl groups were employed to generate diamond nanowire/nanotubes [18]. The diamondoids are NEA material [1], which can be driven to the cathode in the direct current (DC) electrical field, whereas the AAO is a Lewis acid [36]. Therefore, a reasonable mechanism may be as follows in this article. In the first step, the NEA nature of the diamondoid may lead them to the cathode under the DC electric field. Second, the

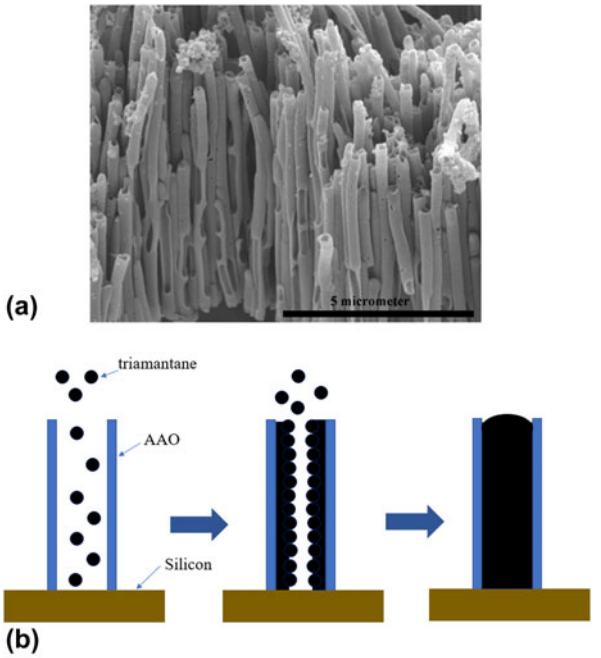


Figure 3: (a) SEM images of diamondoid nanowires and (b) mechanism of diamondoid nanowire fabrication.

diamondoid may be ready to be ionized in acetonitrile to generate H^+, and these ionized diamondoid may be easy to attach onto the AAO surface walls by electrostatic force. At last, with increasing fabrication, the diamondoid may continuously attach onto formed diamondoid surface wall to finally build diamondoid nanowires.

Surprisingly, clear hierarchical branched diamondoid nanowires were found in SEM image. As shown in Fig. 4(a), the diamondoid nanowires presented hierarchical branched nanostructure that was similar to the novel metal nanowires or

https://doi.org/10.1557/jmr.2019.197 Published online by Cambridge University Press

© Materials Research Society 2019

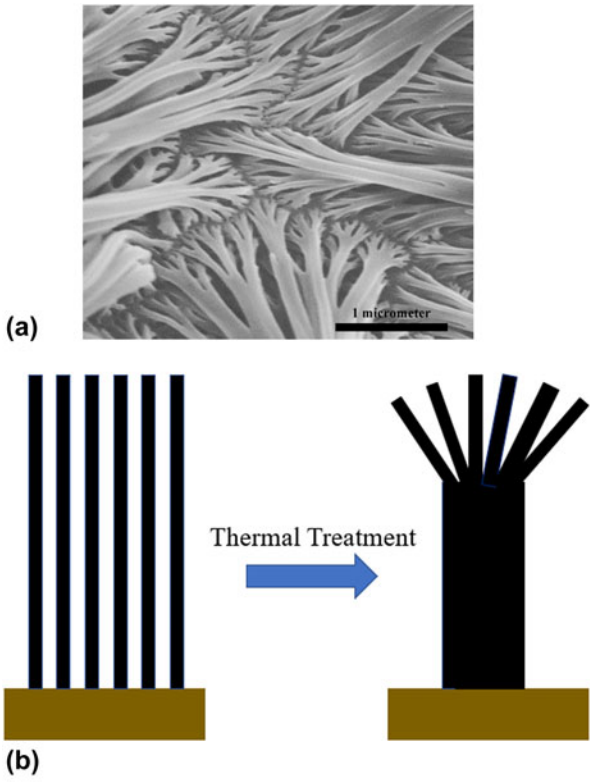


Figure 4: (a) SEM images of hierarchical branched diamondoid nanowire and (b) schematic figure of hierarchical branched diamondoid nanowire formation.

silicon nanotubes in previous publications [29]. Chen et al. produced branched silicon nanotubes and metal nanowires via AAO-template–assistant approach, in which the AAO template was fabricated in a complicated process. In addition, Kumar's group achieved branched metallic glass nanowire via hierarchical patterning [29]. The above methods to produce the branched nanowires had understanding disadvantages, complicated manufacturing, high cost, etc. However, in this method, the hierarchical branched diamondoid nanowires were fabricated via a facile two-step approach, including cathodic EPD and thermal treatment, which is much simpler compared to abovementioned manufacturing process. These hierarchical branched diamondoid nanowires were found at the interface between the nanowires array and the silicon substrate. The diameter of these hierarchical branched diamondoid nanowires at bottom was sum of diameter of branches at the top of diamondoid nanowires, which the top of these hierarchical branched diamondoid nanowires had a uniform diameter around 200 nm, which is the diameter of single diamondoid nanowire. These results demonstrate that the hierarchical branched diamondoid nanowires are combined of several diamondoid nanowires with an integrated diamondoid nanowire at bottom and a few separated diamondoid nanowires at top. As presented in Fig. 4(b), a thermal treatment around 241.5 °C, which is much higher than the melting point of triamantane, was employed to improve the mechanical properties of diamondoid nanowires array. During this heating treatment, the triamantane was melted and combined together at the bottom of diamondoid nanowires, whereas the top of diamondoid nanowires was easy to collapse due to poor mechanical properties, which make them hard to contact each other to combine them together. After thermal treatment, the diamondoid nanowires at bottom were combined to be an integrated nanowire. On the other hand, the diamondoid nanowires at top were cooled to form branched diamondoid nanowires. To well understand the formation of hierarchical branched diamondoid nanowire during thermal treatment, a systematical experiment will be performed in detail and the mechanism of hierarchical branched diamondoid nanowire will be presented in the following article.

Conclusion

In this article, hierarchical branched diamondoid nanostructures were fabricated via a facile approach combining cathodic EPD and two-step thermal treatment. Triamantane was employed as raw material to achieve diamondoid nanowires via porous AAO film, and vertical diamondoid nanowires were achieved after critical point drying. A two-step thermal treatment was applied to achieve hierarchical branched diamondoid nanowires array, which might open a new approach to fabricate novel nanostructure array. In addition, the mechanism of diamondoid nanowire/nanotube formation and hierarchical branched diamondoid nanowires formation were introduced.

Methodology

In the present study, triamantane, three-cage diamondoids, were used to produce diamondoid nanostructures. It was obtained from the higher diamondoids discovered by Dr. Jeremy Dahl. Anhydrous toluene (99.8%) was purchased from Sigma Aldrich (Burlington, MA). Commercial AAO film was ordered from Whatman Ltd (Pittsburgh, PA). The size of AAO pore is around 200 nm and the thickness of AAO film is around 60 μm. Series 2400 SourceMeter from Keithley Instrument, Inc. (Beaverton, OR), was used to control the electrophoresis process.

10 mg triamantane was dissolved in 20 mL toluene by a bath sonication for 15 min. At the same time, AAO film was attached to a silicon wafer by Ag/epoxy conductive binder, which was used as a working electrode. The diced silicon substrates were first achieved by a glass knife and were cleaned by a mixture solution consisting of NH_4OH (20% solution), H_2O_2 (30% solution), and deionized water (DI water) with a ratio at 5:1:1 and heated around 60 °C for 3 h. After that, these diced silicon substrates were rinsed with DI water and

https://doi.org/10.1557/jmr.2019.197 Published online by Cambridge University Press

© Materials Research Society 2019

dried at 70 °C under a nitrogen atmosphere, and then were stored in desiccators before using [5]. This silicon/AAO–based working electrode was assembled onto the cathode, and a platinum wire was used on the anode as a counter electrode. Then both anode and cathode were put into the toluene solution. During the cathodic electrophoretic deposition, a Series 2400 SourceMeter from Keithley Instrument, Inc., was used as a power source, and the voltage was 30 V and current was 1 mA (as shown in Fig. S1). The distance between the cathode and anode was 1 cm.

After 1 h, the silicon wafer was transferred into 1 mol/L sodium hydroxide solution to remove the AAO template for another 1 h. However, the nanowires obtained in this way laid on the substrate randomly. To achieve vertically aligned diamondoid nanowire arrays, critical point drying method was applied. The AAO template adhered to silicon wafer was first etched by sodium hydroxide solution and then rinsed with DI water and ethanol mixture (90/10, 70/30, 50/50, 30/70, 20/80, 10/90, and 0/100) for 15 min to remove water, respectively. Finally, the vertically aligned diamondoid nanowire arrays were achieved by removing ethanol via the supercritical point drying technique. To well improve the mechanical properties of diamondoid nanowires, two various heat treatment processes were employed, including a one-step method and a two-step method. In the one-step method, the diamondoid nanowire array was heated up to 226.5 °C for 1 h. This temperature (226.5 °C) is little higher than the melting point of triamantane [35]. On the other hand, in the two-step method, the diamondoid nanowire array was first heated at 241.5 °C for 2 h and cooled down in the oven. At the second stage, the diamondoid nanowire array was heated at 141.5 °C to remove the residual stress.

Differential scanning calorimetry (DSC) was performed on a TA Q20 (TA Instruments, Inc.) with a heating rate of 2 °C/min to analysis thermodynamic properties of triamantane. In addition, all the nanowire arrays were characterized by scanning electron microscopy (SEM), which were performed on Hitachi S-570 and S-4300 (Hitachi Appliances Inc., Japan). Before operating on the Hitachi S-570 and S-4300, all the nanowire arrays were coated with Au film by a sputter coating instrument.

Acknowledgment

The authors would like to acknowledge the support from National Science Foundation (NSF) Grant No. 1228127. The authors would like to thank the imaging center in Texas Tech University for SEM imaging.

Supplementary material

To view supplementary material for this article, please visit https://doi.org/10.1557/jmr.2019.197.

References

1. **S. Roth, D. Leuenberger, J. Osterwalder, J.E. Dahl, R.M.K. Carlson, B.A. Tkachenko, A.A. Fokin, P.R. Schreiner, and M. Hengsberger**: Negative-electron-affinity diamondoid monolayers as high-brilliance source for ultrashort electron pulses. *Chem. Phys. Lett.* **495**, 102–108 (2010).
2. **D. He, X. Huang, and M.Q. Li**: Hierarchical C–P(=O)(–O–)$_n$ ($n \leq 2$)-linked nano-Si/N-doped C/graphene porous foam as anodes for high-performance lithium ion batteries. *Carbon* **141**, 531–541 (2019).
3. **X. Zhang, K.S. Ziemer, K. Zhang, D. Ramirez, L. Li, S.R. Wang, L.J. Hope-Weeks, and B.L. Weeks**: Large-area preparation of high-quality and uniform three-dimensional graphene networks through thermal degradation of graphene oxide-nitrocellulose composites. *ACS Appl. Mater. Interfaces* **7**, 1057–1064 (2015).
4. **X. Zhang, W.M. Hikal, Y. Zhang, S.K. Bhattacharia, L. Li, S. Panditrao, S.R. Wang, and B.L. Weeks**: Direct laser initiation and improved thermal stability of nitrocellulose/graphene oxide nanocomposites. *Appl. Phys. Lett.* **102**, 141905 (2013).
5. **X. Zhang, X. Ji, R.F. Su, B.L. Weeks, Z. Zhang, and S.L. Deng**: Aerobic oxidation of 9H-fluorenes to 9-fluorenones using mono-/multilayer graphene-supported alkaline catalyst. *Chempluschem* **78**, 703–711 (2013).
6. **G. Zhang**: Diamondoid molecules: With applications in biomedicine, materials science, nanotechnology and petroleum science. *Phys. Today* **66**, 59–60 (2013).
7. **J.R. Schnell and J.J. Chou**: Structure and mechanism of the M2 proton channel of influenza A virus. *Nature* **451**, 591–U12 (2008).
8. **M. Fyta**: Stable boron nitride diamondoids as nanoscale materials. *Nanotechnology* **25**, 365601 (2014).
9. **R. Richter, D. Wolter, T. Zimmermann, L. Landt, A. Knecht, C. Heidrich, A. Merli, O. Dopfer, P. Reiss, A. Ehresmann, J. Petersen, J.E. Dahl, R.M.K. Carlson, C. Bostedt, T. Moller, R. Mitric, and T. Rander**: Size and shape dependent photoluminescence and excited state decay rates of diamondoids. *Phys. Chem. Chem. Phys.* **16**, 3070–3076 (2014).
10. **Y. Xue and G.A. Mansoori**: Self-Assembly of diamondoid molecules and derivatives (MD simulations and DFT calculations). *Int. J. Mol. Sci.* **11**, 288–303 (2010).
11. **R.C. Fort and P.V. Schleyer**: Adamantane: Consequences of diamondoid structure. *Chem. Rev.* **64**, 277–300 (1964).
12. **Y.J. Zhou, A.D. Brittain, D.Y. Kong, M. Xiao, Y.Z. Meng, and L.Y. Sun**: Derivatization of diamondoids for functional applications. *J. Mater. Chem. C* **3**, 6947–6961 (2015).
13. **J.E. Dahl, S.G. Liu, and R.M.K. Carlson**: Isolation and structure of higher diamondoids, nanometer-sized diamond molecules. *Science* **299**, 96–99 (2003).
14. **H.B. Lu, X. Wang, Y.T. Yao, J.H. Gou, D. Hui, B. Xu, and Y.Q. Fu**: Synergistic effect of siloxane modified aluminum nanopowders and carbon fiber on electrothermal efficiency of

https://doi.org/10.1557/jmr.2019.197 Published online by Cambridge University Press

© Materials Research Society 2019

polymeric shape memory nanocomposite. *Composites, Part B* **80**, 1–6 (2015).

15. **J.R. Choi, K.Y. Rhee, and S.J. Park**: Influence of electrolessly silver-plated multi-walled carbon nanotubes on thermal conductivity of epoxy matrix nanocomposites. *Composites, Part B* **80**, 379–384 (2015).
16. **Y. Yamamoto, T. Fukushima, Y. Suna, N. Ishii, A. Saeki, S. Seki, S. Tagawa, M. Taniguchi, T. Kawai, and T. Aida**: Photoconductive coaxial nanotubes of molecularly connected electron donor and acceptor layers. *Science* **314**, 1761–1764 (2006).
17. **L. Jiang, H.L. Dong, Q. Meng, H.X. Li, M. He, Z.M. Wei, Y.D. He, and W.P. Hu**: Millimeter-sized molecular monolayer two-dimensional crystals. *Adv. Mater.* **23**, 2059–2063 (2011).
18. **L. Li, K. Zhang, J.J. Qiu, S.R. Wang, H.H. Van, and M. Zhang**: Solution assembly of vertically aligned diamond nanotube arrays from diamond nanocrystals. *Diamond Relat. Mater.* **29**, 79–83 (2012).
19. **W. Janssen and E. Gheeraert**: Dry etching of diamond nanowires using self-organized metal droplet masks. *Diamond Relat. Mater.* **20**, 389–394 (2011).
20. **C.H. Hsu, S.G. Cloutier, S. Palefsky, and J. Xu**: Synthesis of diamond nanowires using atmospheric-pressure chemical vapor deposition. *Nano Lett.* **10**, 3272–3276 (2010).
21. **M.Q. Zhao, C.E. Ren, Z. Ling, M.R. Lukatskaya, C.F. Zhang, K.L. Van Aken, M.W. Barsoum, and Y. Gogotsi**: Flexible MXene/carbon nanotube composite paper with high volumetric capacitance. *Adv. Mater.* **27**, 339–345 (2015).
22. **X.W. Mao, F. Simeon, G.C. Rutledge, and T.A. Hatton**: Electrospun carbon nanofiber webs with controlled density of states for sensor applications. *Adv. Mater.* **25**, 1309–1314 (2013).
23. **U. Chandni, P. Kundu, S. Kundu, N. Ravishankar, and A. Ghosh**: Tunability of electronic states in ultrathin gold nanowires. *Adv. Mater.* **25**, 2486–2491 (2013).
24. **X. Zhang, Y. He, M.L. Sushko, J. Liu, L.L. Luo, J.J. De Yoreo, S.X. Mao, C.M. Wang, and K.M. Rosso**: Direction-specific van der Waals attraction between rutile TiO_2 nanocrystals. *Science* **356**, 434–437 (2017).
25. **X. Zhang, Z. Shen, J. Liu, S.N. Kerisit, M.E. Bowden, M.L. Sushko, J.J. De Yoreo, and K.M. Rosso**: Direction-specific interaction forces underlying zinc oxide crystal growth by oriented attachment. *Nat. Commun.* **8**, 835 (2017).
26. **B.P. Singh, S. Nayak, K.K. Nanda, B.K. Jena, S. Bhattacharjee, and L. Besra**: The production of a corrosion resistant graphene reinforced composite coating on copper by electrophoretic deposition. *Carbon* **61**, 47–56 (2013).
27. **S.J. Limmer, S. Seraji, Y. Wu, T.P. Chou, C. Nguyen, and G.Z. Cao**: Template-based growth of various oxide nanorods by sol–gel electrophoresis. *Adv. Funct. Mater.* **12**, 59–64 (2002).
28. **E.Y. Ye, M.D. Regulacio, S.Y. Zhang, X.J. Loh, and M.Y. Han**: Anisotropically branched metal nanostructures. *Chem. Soc. Rev.* **44**, 6001–6017 (2015).
29. **M. Hasan, J. Schroers, and G. Kumar**: Functionalization of metallic glasses through hierarchical patterning. *Nano Lett.* **15**, 963–968 (2015).
30. **K.T. Narasimha, C.H. Ge, J.D. Fabbri, W. Clay, B.A. Tkachenko, A.A. Fokin, P.R. Schreiner, J.E. Dahl, R.M.K. Carlson, Z.X. Shen, and N.A. Melosh**: Ultralow effective work function surfaces using diamondoid monolayers. *Nat. Nanotechnol.* **11**, 267–272 (2016).
31. **H. Yan, J.N. Hohman, F.H. Li, C.J. Jia, D. Solis-Ibarra, B. Wu, J.E.P. Dahl, R.M.K. Carlson, B.A. Tkachenko, A.A. Fokin, P.R. Schreiner, A. Vailionis, T.R. Kim, T.P. Devereaux, Z.X. Shen, and N.A. Melosh**: Hybrid metal-organic chalcogenide nanowires with electrically conductive inorganic core through diamondoid-directed assembly. *Nat. Mater.* **16**, 349–355 (2017).
32. **C.S. Sarap, P. Partovi-Azar, and M. Fyta**: Enhancing the optical detection of mutants from healthy DNA with diamondoids. *J. Mater. Chem. B* **7**, 3424–3430 (2019).
33. **C.S. Sarap, P. Partovi-Azar, and M. Fyta**: Optoelectronic properties of diamondoid-DNA complexes. *ACS Appl. Bio Mater.* **1**, 59–69 (2018).
34. **Y. Zhang, C.W. Lo, J.A. Taylor, and S. Yang**: Replica molding of high-aspect-ratio polymeric nanopillar arrays with high fidelity. *Langmuir* **22**, 8595–8601 (2006).
35. **G.A. Mansoori**: Diamondoid molecules. *Adv. Chem. Phys.* **136**, 207–258 (2007).
36. **H.Q. Cao, Y. Xu, J.M. Hong, H.B. Liu, G. Yin, B.L. Li, C.Y. Tie, and Z. Xu**: Sol–gel template synthesis of an array of single crystal CdS nanowires on a porous alumina template. *Adv. Mater.* **13**, 1393–1394 (2001).

https://doi.org/10.1557/jmr.2019.197 Published online by Cambridge University Press

© Materials Research Society 2019